

## DECLARATION

I declare that the thesis entitled “**APPLICATION OF METALLIC NANOCHITOSAN AGAINST POST-HARVEST FUNGAL PATHOGENS OF WHEAT AND ELICITATION OF RESISTANCE BY SOLID MATRIX PRIMING**” has been completed by me under the supervision of Dr. Piyush Mathur and co-supervision of Dr. Chandrani Choudhuri. This thesis contains authentic research and informations. The work done in this thesis has significant values in the field of agriculture. No part of this thesis has formed the basis for the award of any degree or fellowship previously.

Date: 23.07.2024

*Divya Chouhan*  
**DIVYA CHOUHAN**

UGC-NET SRF  
Department of Botany,  
University of North Bengal,  
Raja Rammohunpur, Siliguri  
West Bengal, India-734013



**DR. PIYUSH MATHUR**  
Assistant Professor  
Department of Botany  
University of North Bengal

### CERTIFICATE

This is to certify that the thesis entitled “APPLICATION OF METALLIC NANOCHITOSAN AGAINST POST-HARVEST FUNGAL PATHOGENS OF WHEAT AND ELICITATION OF RESISTANCE BY SOLID MATRIX PRIMING” submitted by **Ms. Divya Chouhan** for the award of the degree of Doctor of Philosophy in Botany is based on the results of experiments carried out by her. She has worked under my supervision at Department of Botany, University of North Bengal. I am forwarding her thesis for the award of Ph.D. Degree under University of North Bengal. She has fulfilled all requirements according to the rules of the University of North Bengal regarding the works embodied in her thesis.

**DR. PIYUSH MATHUR**

Assistant Professor  
Department of Botany  
University of North Bengal

**Dr. PIYUSH MATHUR**

Assistant Professor  
Department of Botany  
University of North Bengal  
Raja Rammohunpur, Distt. Darjeeling,  
Bengal - 734013



**DR. CHANDRANI CHOUDHURI**

Date: 02.07.2024

Assistant Professor  
Department of Botany  
North Bengal St. Xavier's College, Jalpaiguri

### CERTIFICATE

This is to certify that the thesis, entitled “APPLICATION OF METALLIC NANOCHITOSAN AGAINST POST-HARVEST FUNGAL PATHOGENS OF WHEAT AND ELICITATION OF RESISTANCE BY SOLID MATRIX PRIMING” embodies the results of the work conducted by Ms. Divya Chouhan for the award of degree of Doctor of Philosophy in Botany under my co-supervision. She has carried out the work at the Department of Botany, University of North Bengal. I am forwarding herewith her thesis for the award of Ph.D. degree in Science (Botany), University of North Bengal.

*Chandrani Choudhuri*  
**DR. CHANDRANI CHOUDHURI**

Assistant Professor, HOD  
Department of Botany  
North Bengal St. Xavier's College

**Dr. Chandrani Choudhuri**  
Assistant Professor  
Dept. of Botany  
North Bengal St. Xavier's College



## DRC CERTIFICATE

It is certified that the work contained in the thesis titled "APPLICATION OF METALLIC NANOCHITOSAN AGAINST POST - HARVEST FUNGAL PATHOGENS OF WHEAT AND ELICITATION OF RESISTANCE BY SOLID MATRIX PRIMING" has been carried out following University guideline and it has been approved by the members present in the meeting of the Departmental Research Committee in Botany for processing by the Board of Research Studies.

Approved

Date:

Prof. Arnab Sen .....

Name and Signature of DRC (Member)

Prof. Arnab Sen  
Department of Botany  
University of North Bengal

Prof. Subhas Chandra Roy .....

Name and Signature of DRC (Member)

Dr. Monoranjan  
Professor  
Department of E  
University of North Bengal

Prof. Monoranjan Chowdhury .....

Name and Signature of DRC (Member)

Dr. Swarnendu Roy .....

Name and Signature of DRC (Member)

Dr. Swarnendu Roy  
Assistant Professor  
Department of Botany  
University of North Bengal  
Raja Rammohunpur, Pin-734013

Dr. Piyush Mathur .....

Name and Signature of DRC (Member)

Dr. PIYUSH MATHUR  
Assistant Professor  
Department of Botany  
University of North Bengal  
Raja Rammohunpur, Distt. Darj  
West Bengal - 734013

Name of the Chairperson of DRC:

Prof. Aniruddha Saha

Full signature of the chairperson.....

Aniruddha Saha

Aniruddha Saha

Head

Department of Botany  
North Bengal University  
Prof. Aniruddha Saha  
Professor & Head  
Department of Botany  
University of North Bengal

**Submission Information**

Author Name Divya Chouhan  
Title APPLICATION OF METALLIC NANOCHITOSAN AGAINST POST-HARVEST FUNGAL PATHOGENS OF WHEAT AND ELICITATION OF RESISTANCE BY SOLID MATRIX PRIMING  
Paper/Submission ID 2075288  
Submitted by nbuplg@nbu.ac.in  
Submission Date 2024-07-03 10:58:36  
Total Pages, Total Words 305, 66956  
Document type Thesis

**Result Information**Similarity **0 %**

0 10 20 30 40 50 60 70 80 90 100

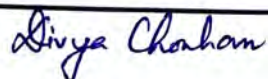
**Exclude Information**

Quotes Excluded  
References/Bibliography Excluded  
Source: Excluded < 14 Words Excluded  
Excluded Source 3 %  
Excluded Phrases Not Excluded

**Database Selection**

Language English  
Student Papers Yes  
Journals & publishers Yes  
Internet or Web Yes  
Institution Repository Yes

A Unique QR Code use to View/Download/Share Pdf File

**Dr. PIYUSH MATHUR**

Assistant Professor  
Department of Botany  
University of North Bengal  
Darjeeling, Distt. Darjeeling  
West Bengal - 734013  
Phone: 0354-2734013

*Dedicated to...*

*This thesis is wholeheartedly dedicated to my former supervisor, Late Dr. Palash Mandal Sir, who has been my source of inspiration, all time. His absence is very painful for me.*

## *Acknowledgement*

It takes severe patience and enormous hard work to complete a Ph.D. thesis. I am grateful to numerous peers who have contributed to this research work. First and foremost, I would like to express my gratitude towards my former supervisor, the Late Dr. Palash Mandal Sir who inculcated me with the urge to pursue research in this stream. It is very painful for me to end my thesis in his absence.

I am thankful to my supervisor Dr. Piyush Mathur Sir, who made a constant stream of support and motivation during my research tenure. His valuable advice and comments have encouraged me to study every topic of research in-depth and thus helped me to complete my work with finesse. I thank him for providing me with the opportunity to work with him.

I am grateful to my co-supervisor Dr. Chandrani Choudhuri Madam for providing constant motivation, support, and sincere guidance not only in the field of research but also in life relations. Her observations and comments helped me to draw the overall direction of the research and to move forward with in-depth investigations.

I am also grateful to all the former Heads of this department during the tenure of my research work for providing me with all the requirements and facilities.

I am thankful to Prof. Aniruddha Saha, present Head of the Department of Botany, for providing me with all the research-related assistance and facilities. I would also like to thank all the faculty members of Department of Botany, namely Prof. A. Sen, Prof S.C. Roy, Prof. M. Chowdhury, and Dr. S. Roy for their support, help, and encouragement.

I express my heartfelt gratitude towards every non-teaching staff of the department for their help in different ways.

I thank University Grant Commission (Government of India) for providing UGC-NET JRF Fellowship (672/CSIRNET JUNE 2019). I am grateful to DST-FIST facility, Department of Botany (Sanc. No. SR/FST/LS-I/2021/900) for all instrumentation facilities. I am highly grateful to the University of North Bengal for providing the necessary research support. I am also thankful to National Seeds Corp. Ltd., New Delhi, SAIF-IIT Bombay, IIT-Madras, CIF-Lovely Professional University, India and USIC, NBU for their assistance and cooperation. I thank the regional substation of UBKV, Khoribari for sharing their knowledge in this field.

I pay my sincere gratitude to Dr. Anoop Kumar Sir and Mrs. Ankita Dutta, Department of Biotechnology, NBU for assisting me in conducting a few experiments of my research. I am thankful to Mr. Debojit Dutta, Department of Zoology for rendering me instrumentation support during my research tenure.

Teamwork is an important factor while working in a laboratory for long five years. I have been fortunate to work with an amazing team of researchers in Nanobiology and Phytotherapy Research Laboratory and Microbiology Laboratory of this University. I am thankful to Dr. Sujoy Kumar Sen, Department of Botany, Siliguri College, for helping me learning research-related things. I am thankful to Dr. Dipayan Das for his sincere guidance. A special vote of thanks to Mr. Kushankur Sarkar for his support, help and encouragement. I express my love to Dr. Arunika Subba and Ms. Suravi Ghosh for being a great companion in the lab. I am grateful to Ms. Prabha Toppo for her support and the emotional bonding that she had shared with me. I thank Mr. Debmallya Pathak and Mr. Rewaj Subba of Microbiology Laboratory, for their constant help and moral support.

I express my sincere love and gratitude to my supportive family, especially my mother Mrs. Chanda Chouhan and my mother-in-law Mrs. Beauty Kar, who have been a constant ray of hope in every of my hard situations.

## LIST OF TABLES

Table no.	Table legend	Page no.
Table 2.1	Summarization of different nanomaterials used against various seed-borne pathogens derived from wheat and other cereal crops.	14-15
Table 2.2	Anti-pathogenic activity of chitosan under differential features.	24-25
Table 3.1	Encapsulation efficiency % and particle yield of the synthesized nanoparticles.	55
Table 4.1	Morphological detection of various abnormalities observed in five wheat cultivars.	74
Table 4.2	Identified fungal species isolated from five cultivars of wheat seeds with their authentic I.D. numbers.	75
Table 4.3	List of isolated seed-borne fungal pathogens through blotter paper and agar plate method.	77
Table 4.4	Frequency percentage of the isolated seed-borne pathogens observed in five wheat cultivars.	78
Table 4.5	Relative abundance of the isolated seed-borne pathogens observed in five wheat cultivars.	79
Table 4.6	Disease development caused by seed-borne pathogens on wheat seeds during pathogenicity test.	80
Table 5.1	Tabulation of differential treatments on five different wheat cultivars through nano-priming approach under pathogenic stress.	129
Table 5.2	Effect of solid matrix priming with different metallic nanochitosan, on germination attributes of wheat cultivars, under <i>A. flavus</i> inoculated and uninoculated condition.	139
Table 5.3	Changes in antioxidant enzymological attributes of nano-primed seeds of five different wheat cultivars, under <i>A. flavus</i> inoculated and uninoculated condition.	151
Table 5.4	Categorization of the cultivars on the basis of disease development % under non-primed condition and artificially inoculated with <i>A. flavus</i> .	156
Table 6.1	Tabulation of differential treatments on wheat seeds through nano-priming approach under pathogenic stress.	171

---

Table 7.1	Treatments on wheat seeds through nano-priming approach under pathogenic stress. * denote the presence of <i>A. flavus</i> .	232
Table 7.2	Effect of solid matrix priming with Ag-CNPs, in comparison with CNPs and non-primed seeds, on germination attributes of three wheat cultivars, under <i>A. flavus</i> inoculated and uninoculated condition.	246
Table 7.3	List of 29 metabolites detected in non-primed harvested seeds of HI 8759 cultivar by LC-MS analysis.	281-282
Table 7.4	List of 55 metabolites detected in Ag-CNPs primed harvested seeds of HI 8759 cultivar by LC-MS analysis.	282-284

---

## LIST OF FIGURES

Figure no.	Figure legend	Page no.
Fig. 2.1	State-wise production of wheat in India in the last financial year of 2022-2023, according to the Ministry of Agriculture and Farmers Welfare.	7
Fig. 2.2	Absolute increase/decrease in the production of wheat in India, in the last financial year of 2022-2023, according to Ministry of Agriculture and Farmers Welfare.	8
Fig. 2.3	Seed-borne disease of wheat caused during post-harvest condition.	10
Fig. 2.4	Aspects of nanotechnology in modern day agricultural system.	14
Fig. 2.5	Production of chitin from crustaceans and chitosan from chitin.	15
Fig. 2.6	Various implications of chitosan nano-derivatives on crop system.	16
Fig. 2.7	Synthesis of chitosan nanoparticles through ionotropic gelation method.	20
Fig. 2.8	Structural configuration of (a) Silver nano-chitosan, (b) Copper nano-chitosan and (c) Zinc nano-chitosan.	21
Fig. 2.9	Mechanism of action of chitosan nano-derivatives on Gram-positive and Gram-negative bacteria.	26
Fig. 2.10	Mechanism of action of chitosan nano-derivatives on fungi.	27
Fig. 2.11	Effect of seed nano-priming on seed biochemistry and physiology.	29
Fig. 3.1	Nano-hydrogel images and synthesis of (a) CNPs, (b) Ag-CNPs, (c) Ni-CNPs, (d) Cu-CNPs, (e) Zn-CNPs and (f) Fe-CNPs through Ionic Gelation Method.	39
Fig. 3.2	UV-vis spectra of (a) CNPs, (b) Ag-CNPs, (c) Ni-CNPs, (d) Cu-CNPs, (e) Zn-CNPs and (f) Fe-CNPs.	41
Fig. 3.3	FE-SEM analysis images of (a) CNPs, (b) Ag-CNPs, (c) Ni-CNPs, (d) Cu-CNPs, (e) Zn-CNPs and (f) Fe-CNPs.	42

Fig. 3.4	EDXS analysis of (a) CNPs, (b) Ag-CNPs, (c) Ni-CNPs, (d) Cu-CNPs, (e) Zn-CNPs and (f) Fe-CNPs.	44
Fig. 3.5	HR-TEM images of (a) CNPs, (b) Ag-CNPs, (c) Ni-CNPs, (d) Cu-CNPs, (e) Zn-CNPs and (f) Fe-CNPs.	45
Fig. 3.6	Size distribution histogram of (a) CNPs, (b) Ag-CNPs, (c) Ni-CNPs, (d) Cu-CNPs, (e) Zn-CNPs and (f) Fe-CNPs.	46
Fig. 3.7	FT-IR analysis of CNPs.	47
Fig. 3.8	FT-IR analysis of Ag-CNPs.	48
Fig. 3.9	FT-IR analysis of Ni-CNPs.	48
Fig. 3.10	FT-IR analysis of Cu-CNPs.	49
Fig. 3.11	FT-IR analysis of Zn-CNPs.	49
Fig. 3.12	FT-IR analysis of Fe-CNPs.	50
Fig. 3.13	DLS analysis of (a) CNPs, (b) Ag-CNPs, (c) Ni-CNPs, (d) Cu-CNPs, (e) Zn-CNPs and (f) Fe-CNPs.	51
Fig. 3.14	Zeta-potential analysis of (a) CNPs, (b) Ag-CNPs, (c) Ni-CNPs, (d) Cu-CNPs, (e) Zn-CNPs and (f) Fe-CNPs.	52
Fig. 3.15	Laser ablation of (a) CNPs, (b) Ag-CNPs, (c) Ni-CNPs, (d) Cu-CNPs, (e) Zn-CNPs and (f) Fe-CNPs through Tyndall effect.	53
Fig. 3.16	Swelling index of synthesized nanoparticles on the basis of 0, 1, 2, 3, 4, 5 and 6 hours.	54
<hr/>		
Fig. 4.1	Infected wheat seeds of Sonalika, PBW 343, DBW 187, HD 2679 and HI 8759, collected from local seed preservatories.	65
Fig. 4.2	Isolation of seed-borne fungal pathogens from (a) infected wheat seeds through (b-c) agar plate method and (d-e) blotter paper technique.	67
Fig. 4.3	Pathogenicity test on healthy wheat seeds through (a) seed injury with sterilized needle under laminar air flow, followed by (b) inoculation of fungal inoculum in seeds through sterilized inoculation loop.	68
Fig. 4.4	Microscopic observation of ten isolated seed-borne pathogens of wheat (a) <i>Curvularia pallescens</i> , (b) <i>Aspergillus fumigatus</i> , (c) <i>Rhizopus stolonifer</i> , (d) <i>Penicillium chrysogenum</i> , (e) <i>A.</i>	76

	<i>flavus</i> , (f) <i>A. niger</i> , (g) <i>Fusarium oxysporum</i> , (h) <i>F. solani</i> , (i) <i>Cladosporium cladosporioides</i> and (j) <i>Alternaria triticina</i> .	
Fig. 4.5	Pathogenicity test performed on fresh wheat seeds by artificial inoculation of (a) <i>Rhizopus stolonifer</i> , (b) <i>Aspergillus flavus</i> , (c) <i>A. niger</i> , (d) <i>Curvularia pallescens</i> , (e) <i>Fusarium solani</i> , (f) <i>A. fumigatus</i> , (g) <i>F. oxysporum</i> , (h) <i>Penicillium chrysogenum</i> , (i) <i>Cladosporium cladosporioides</i> and (j) <i>Alternaria triticina</i> through standard blotter technique.	81
Fig. 4.6	Effect of different metallic nanochitosan on mycelium radial growth of <i>Aspergillus flavus</i> , in comparison with CNPs and control under the concentration range of 100-500 µg/mL.	84
Fig. 4.7	Effect of different metallic nanochitosan on (a) colony diameter and (b) percent inhibition of radial growth (PIRG) % of <i>A. flavus</i> .	85
Fig. 4.8	Effect of different metallic nanochitosan on mycelium radial growth of <i>Aspergillus niger</i> , in comparison with CNPs and control under the concentration range of 100-500 µg/mL.	86
Fig. 4.9	Effect of different metallic nanochitosan on (a) colony diameter and (b) percent inhibition of radial growth (PIRG) % of <i>A. niger</i> .	87
Fig. 4.10	Effect of different metallic nanochitosan on mycelium radial growth of <i>Curvularia pallescens</i> , in comparison with CNPs and control under the concentration range of 100-500 µg/mL.	88
Fig. 4.11	Effect of different metallic nanochitosan on (a) colony diameter and (b) percent inhibition of radial growth (PIRG) % of <i>C. pallescens</i> .	89
Fig. 4.12	Effect of different metallic nanochitosan on mycelium radial growth of <i>Fusarium solani</i> , in comparison with CNPs and control under the concentration range of 100-500 µg/mL.	90
Fig. 4.13	Effect of different metallic nanochitosan on (a) colony diameter and (b) percent inhibition of radial growth (PIRG) % of <i>F. solani</i> .	91

Fig. 4.14	Effect of Ni-CNPs on (a) colony diameter and (b) percent inhibition of radial growth (PIRG) % of <i>F. solani</i> .	92
Fig. 4.15	Effect of different metallic nanochitosan on mycelium radial growth of <i>Penicillium chrysogenum</i> , in comparison with CNPs and control under the concentration range of 100-500 µg/mL.	93
Fig. 4.16	Effect of different metallic nanochitosan on (a) colony diameter and (b) percent inhibition of radial growth (PIRG) % of <i>P. chrysogenum</i> .	94
Fig. 4.17	Effect of different metallic nanochitosan on mycelium radial growth of <i>Rhizopus stolonifer</i> , in comparison with CNPs and control under the concentration range of 100-500 µg/mL.	95
Fig. 4.18	Effect of different metallic nanochitosan on (a) colony diameter and (b) percent inhibition of radial growth (PIRG) % of <i>R. stolonifer</i> .	96
Fig. 4.19	IC50 value of different metallic nanochitosan (Ag-CNPs, Ni-CNPs and Cu-CNPs) and non-metallic CNPs.	97
Fig. 4.20	Screening of seed borne fungal pathogens through spore germination inhibition assay by the application of different metallic nanoparticles at the concentration of 500 µg/mL.	99
Fig. 4.21	Spore germination rate of six high incidence seed-borne pathogens on application of different metallic nanochitosan at the concentration of 500 µg/mL.	100
Fig. 4.22	Spore germination inhibition percentage of six high incidence seed-borne pathogens on application of different metallic nanochitosan at the concentration of 500 µg/mL.	100
Fig. 4.23a	Effect of different metallic nanochitosan on spore viability % of <i>Aspergillus flavus</i> , in comparison with CNPs and control under the concentration range of 100-500 µg/mL.	103
Fig. 4.23b	Effect of different metallic nanochitosan on spore viability % of <i>Fusarium solani</i> , in comparison with CNPs and control under the concentration range of 100-500 µg/mL.	104

Fig. 4.23c	Effect of different metallic nanochitosan on spore viability % of <i>Aspergillus niger</i> , in comparison with CNPs and control under the concentration range of 100-500 µg/mL.	104
Fig. 4.23d	Effect of different metallic nanochitosan on spore viability % of <i>Rhizopus stolonifer</i> , in comparison with CNPs and control under the concentration range of 100-500 µg/mL.	105
Fig. 4.23e	Effect of different metallic nanochitosan on spore viability % of <i>Penicillium chrysogenum</i> , in comparison with CNPs and control under the concentration range of 100-500 µg/mL.	105
Fig. 4.23f	Effect of different metallic nanochitosan on spore viability % of <i>Curvularia pallescens</i> , in comparison with CNPs and control under the concentration range of 100-500 µg/mL.	106
Fig. 4.24	Effect of different metallic nanochitosan on MDA content % of (a) <i>Aspergillus flavus</i> , (b) <i>A. niger</i> , (c) <i>Fusarium solani</i> , (d) <i>Rhizopus stolonifer</i> , (e) <i>Penicillium chrysogenum</i> , and (f) <i>Curvularia pallescens</i> , in comparison with CNPs and control under the concentration range of 100-500 µg/mL.	108-109
Fig. 4.25	Morphological changes in the spore body of <i>F. solani</i> , <i>R. stolonifer</i> , <i>P. chrysogenum</i> , <i>A. flavus</i> , <i>A. niger</i> and <i>C. pallescens</i> due to the effect of Ni-CNPs (40 µg/mL) and Ag-CNPs (500 µg/mL), in comparison with CNPs and control, observed under Scanning Electron Microscopic (SEM).	111
Fig. 4.26	Fluorescence microscopic observations showing generation of oxidative stress in fungal mycelium and spore due to the effect of Ag-CNPs and Ni-CNPs, in comparison with CNPs and control.	113
Fig. 4.27	Localization of metallic core in the chitosan network affirming the configuration of metallic nanochitosan.	123
Fig. 4.28	Mode of action of metallic nanochitosan on fungal pathogen.	123
Fig. 5.1	Healthy seeds of five different cultivars procured from National Seed Corporation Ltd.	126
Fig. 5.2	Representation of seed nano-priming technique followed by seed inoculation with fungal pathogen <i>A. flavus</i> .	128

Fig. 5.3	Effect of solid matrix priming with Ag-CNPs, Cu-CNPs and Ni-CNPs, in comparison with CNPs and non-primed seeds, on five different wheat cultivars, under uninoculated condition.	136
Fig. 5.4	Effect of solid matrix priming with Ag-CNPs, Cu-CNPs and Ni-CNPs, in comparison with CNPs and non-primed seeds, on five different wheat cultivars, under <i>A. flavus</i> inoculated condition.	137
Fig. 5.5	Effect of solid matrix priming with Ag-CNPs, Cu-CNPs and Ni-CNPs, in comparison with CNPs and non-primed seeds, on seed protein composition of Sonalika cultivars, under <i>A. flavus</i> inoculated and uninoculated condition.	141
Fig. 5.6	Seed protein composition of PBW 343 cultivars due to the effect of solid matrix priming with Ag-CNPs, Cu-CNPs and Ni-CNPs, in comparison with CNPs and non-primed seeds, under <i>A. flavus</i> inoculated and uninoculated condition.	141
Fig. 5.7	Effect of solid matrix priming with Ag-CNPs, Cu-CNPs and Ni-CNPs, in comparison with CNPs and non-primed seeds, on seed protein composition of DBW 187 cultivars, under <i>A. flavus</i> inoculated and uninoculated condition.	143
Fig. 5.8	Seed protein composition of HD 2967 cultivars due to the effect of solid matrix priming with Ag-CNPs, Cu-CNPs and Ni-CNPs, in comparison with CNPs and non-primed seeds, under <i>A. flavus</i> inoculated and uninoculated condition.	143
Fig. 5.9	Effect of solid matrix priming with Ag-CNPs, Cu-CNPs and Ni-CNPs, in comparison with CNPs and non-primed seeds, on seed protein composition of HI 8759 cultivars, under <i>A. flavus</i> inoculated and uninoculated condition.	144
Fig. 5.10	Effect of solid matrix priming with Ag-CNPs, Cu-CNPs and Ni-CNPs, in comparison with CNPs and non-primed seeds, on seed carbohydrate composition of Sonalika cultivars, under <i>A. flavus</i> inoculated and uninoculated condition.	146
Fig. 5.11	Seed carbohydrate composition of PBW 343 cultivars due to the effect of solid matrix priming with Ag-CNPs, Cu-CNPs and	146

	Ni-CNPs, in comparison with CNPs and non-primed seeds, under <i>A. flavus</i> inoculated and uninoculated condition.	
Fig. 5.12	Seed carbohydrate composition of DBW 187 cultivars due to the effect of solid matrix priming with Ag-CNPs, Cu-CNPs and Ni-CNPs, in comparison with CNPs and non-primed seeds, under <i>A. flavus</i> inoculated and uninoculated condition.	148
Fig. 5.13	Effect of solid matrix priming with Ag-CNPs, Cu-CNPs and Ni-CNPs, in comparison with CNPs and non-primed seeds, on seed carbohydrate composition of HD 2967 cultivars, under <i>A. flavus</i> inoculated and uninoculated condition.	148
Fig. 5.14	Seed carbohydrate composition of HI 8759 cultivars due to the effect of solid matrix priming with Ag-CNPs, Cu-CNPs and Ni-CNPs, in comparison with CNPs and non-primed seeds, under <i>A. flavus</i> inoculated and uninoculated condition.	149
Fig. 5.15	Effect of solid matrix priming with Ag-CNPs, Cu-CNPs and Ni-CNPs, in comparison with CNPs and non-primed seeds, on disease development % of five wheat cultivars, under <i>A. flavus</i> inoculated condition.	155
Fig. 5.16	Disease development percentage of nano-primed wheat seeds of five different cultivars, under inoculation with <i>A. flavus</i> .	156
Fig. 5.17	Heat map generated for Sonalika cultivar involving germination, seed protein and carbohydrate composition with enzymological attributes in nano-primed wheat seeds.	158
Fig. 5.18	Heat map generated for PBW 343 cultivar involving germination, seed protein and carbohydrate composition with enzymological attributes in nano-primed wheat seeds.	159
Fig. 5.19	Heat map generated for DBW 187 cultivar involving germination, seed protein and carbohydrate composition with enzymological attributes in nano-primed wheat seeds.	160
Fig. 5.20	Heat map generated for HD 2967 cultivar involving germination, seed protein and carbohydrate composition with enzymological attributes in nano-primed wheat seeds.	161

Fig. 5.21	Heat map generated for HI 8759 cultivar involving germination, seed protein and carbohydrate composition with enzymological attributes in nano-primed wheat seeds.	162
<hr/>		
Fig. 6.1	Growth of wheat seedlings of five cultivars after nano-priming of wheat seeds with CNPs and Ag-CNPs, in comparison with the seedlings grown from non-primed seeds, both under <i>A. flavus</i> inoculated and uninoculated condition.	172
Fig. 6.2	Effect of seed nano-priming with Ag-CNPs on (a) seedling height, (b) leaf length, (c) leaf breadth, (d) vigour %, (e) plant height stress tolerance index % and (f) root length stress tolerance index % of Sonalika cultivars, under <i>A. flavus</i> inoculated and uninoculated condition.	181
Fig. 6.3	Analysis of seed nano-priming with Ag-CNPs on (a) seedling height, (b) leaf length, (c) leaf breadth, (d) vigour %, (e) plant height stress tolerance index % and (f) root length stress tolerance index % of PBW 343 cultivars, under <i>A. flavus</i> inoculated and uninoculated condition.	183
Fig. 6.4	Effect of seed nano-priming with Ag-CNPs on (a) seedling height, (b) leaf length, (c) leaf breadth, (d) vigour %, (e) plant height stress tolerance index % and (f) root length stress tolerance index % of DBW 187 cultivars, under <i>A. flavus</i> inoculated and uninoculated condition.	185
Fig. 6.5	Effect of seed nano-priming with Ag-CNPs on (a) seedling height, (b) leaf length, (c) leaf breadth, (d) vigour %, (e) plant height stress tolerance index % and (f) root length stress tolerance index % of HD 2679 cultivars, under <i>A. flavus</i> inoculated and uninoculated condition.	187
Fig. 6.6	Effect of seed nano-priming with Ag-CNPs on (a) seedling height, (b) leaf length, (c) leaf breadth, (d) vigour %, (e) plant height stress tolerance index % and (f) root length stress tolerance index % of HI 8759 cultivars, under <i>A. flavus</i> inoculated and uninoculated condition.	190

Fig. 6.7	Evaluation of total protein content in wheat seedlings due to the priming effect of Ag-CNPs, in comparison with CNPs and non-primed seeds, under <i>A. flavus</i> inoculated and uninoculated condition.	192
Fig. 6.8	Total phenol content in wheat seedlings due to the priming effect of Ag-CNPs, in comparison with CNPs and non-primed seeds, under <i>A. flavus</i> inoculated and uninoculated condition.	194
Fig. 6.9	Total flavonoid content in wheat seedlings due to the priming effect of Ag-CNPs, in comparison with CNPs and non-primed seeds, under <i>A. flavus</i> inoculated and uninoculated condition.	194
Fig. 6.10	Total chlorophyll content in wheat seedlings due to the priming effect of Ag-CNPs, in comparison with CNPs and non-primed seeds, under <i>A. flavus</i> inoculated and uninoculated condition.	197
Fig. 6.11	Total reducing content in wheat seedlings due to the priming effect of Ag-CNPs, in comparison with CNPs and non-primed seeds, under <i>A. flavus</i> inoculated and uninoculated condition.	199
Fig. 6.12	Proline content in wheat seedlings due to the priming effect of Ag-CNPs, in comparison with CNPs and non-primed seeds, under <i>A. flavus</i> inoculated and uninoculated condition.	201
Fig. 6.13	Content of ascorbic acid in wheat seedlings due to the priming effect of Ag-CNPs, in comparison with CNPs and non-primed seeds, under <i>A. flavus</i> inoculated and uninoculated condition.	202
Fig. 6.14	Hydrogen peroxide content in wheat seedlings due to the priming effect of Ag-CNPs, in comparison with CNPs and non-primed seeds, under <i>A. flavus</i> inoculated and uninoculated condition.	203
Fig. 6.15	Catalase activity in wheat seedlings due to the priming effect of Ag-CNPs, in comparison with CNPs and non-primed seeds, under <i>A. flavus</i> inoculated and uninoculated condition.	205
Fig. 6.16	Peroxidase activity in wheat seedlings due to the priming effect of Ag-CNPs, in comparison with CNPs and non-primed seeds, under <i>A. flavus</i> inoculated and uninoculated condition.	207

Fig. 6.17	Superoxide dismutase activity in wheat seedlings due to the priming effect of Ag-CNPs, in comparison with CNPs and non-primed seeds, under <i>A. flavus</i> inoculated and uninoculated condition.	208
Fig. 6.18	Poly phenol oxidase activity in wheat seedlings due to the priming effect of Ag-CNPs, in comparison with CNPs and non-primed seeds, under <i>A. flavus</i> inoculated and uninoculated condition.	210
Fig. 6.19	Ascorbate peroxidase activity in wheat seedlings due to the priming effect of Ag-CNPs, in comparison with CNPs and non-primed seeds, under <i>A. flavus</i> inoculated and uninoculated condition.	211
Fig. 6.20	NADPH oxidase activity in wheat seedlings due to the priming effect of Ag-CNPs, in comparison with CNPs and non-primed seeds, under <i>A. flavus</i> inoculated and uninoculated condition.	212
Fig. 6.21	Phenylalanine ammonia lyase activity in wheat seedlings due to the priming effect of Ag-CNPs, in comparison with CNPs and non-primed seeds, under <i>A. flavus</i> inoculated and uninoculated condition.	214
Fig. 6.22	Tyrosine ammonia lyase activity in wheat seedlings due to the priming effect of Ag-CNPs, in comparison with CNPs and non-primed seeds, under <i>A. flavus</i> inoculated and uninoculated condition.	216
Fig. 6.23	Chitinase activity in wheat seedlings due to the priming effect of Ag-CNPs, in comparison with CNPs and non-primed seeds, under <i>A. flavus</i> inoculated and uninoculated condition.	217
Fig. 6.24	$\beta$ -1,3 glucanases activity in wheat seedlings due to the priming effect of Ag-CNPs, in comparison with CNPs and non-primed seeds, under <i>A. flavus</i> inoculated and uninoculated condition.	219
Fig. 6.25	Comparison of cytotoxicity of CNPs and Ag-CNPs on mammalian kidney HEK293 cells. Cellular toxicity was evaluated based on the percentage of cytotoxicity with different concentrations of CNPs and Ag-CNPs (0.1-2 mg/mL).	220

Fig. 6.26	Comparison of cytotoxicity of CNPs and Cu-CNPs on mammalian kidney HEK293 cells. Cellular toxicity was evaluated based on the percentage of cytotoxicity with different concentrations of CNPs and Ag-CNPs (0.1-2 mg/mL).	220
Fig. 6.27	Comparison of cytotoxicity of CNPs and Cu-CNPs on mammalian kidney HEK293 cells. Cellular toxicity was evaluated based on the percentage of cytotoxicity with different concentrations of CNPs and Ag-CNPs (0.1-2 mg/mL).	221
Fig. 6.28	Mechanistic view of the antioxidant defense response in plant.	223

---

Fig. 7.1	Effect of nano-priming on vegetative growth of pot-grown wheat plants of three cultivars given under agro-net in a completely randomized block design (RBD) at the garden of the Department of Botany, University of North Bengal.	233
Fig. 7.2	Representative wheat plants of (a-c) Sonalika, (d-f) DBW 187 and (g-i) HI 8759 cultivar under treatment with (a,d,g) non-primed plants, (b,e,h) CNPs primed plants and (c,f,i) Ag-CNPs primed plants.	249
Fig. 7.3	Representative wheat plants of (a-c) Sonalika, (d-f) DBW 187 and (g-i) HI 8759 cultivar under treatment with (a,d,g) non-primed plants, (b,e,h) CNPs primed plants and (c,f,i) Ag-CNPs primed plants, inoculated with <i>A. flavus</i> .	250
Fig. 7.4	Effect of Ag-CNPs and CNPs priming on grain/spike of (a) Sonalika, (b) DBW 187 and (c) HI 8759 cultivar, in comparison with non-primed seeds.	251
Fig. 7.5	Effect of Ag-CNPs and CNPs priming on panicle length of (a) Sonalika, (b) DBW 187 and (c) HI 8759 cultivar, in comparison with non-primed seeds.	252
Fig. 7.6	Harvested seeds of (a) Sonalika non-primed, (b) Sonalika non-primed + <i>A. flavus</i> , (c) Sonalika CNPs-primed, (d) Sonalika CNPs-primed + <i>A. flavus</i> , (e) Sonalika Ag-CNPs-primed, (f) Sonalika Ag-CNPs-primed + <i>A. flavus</i> , (g) DBW 187 non-primed, (h) DBW 187 non-primed + <i>A. flavus</i> , (i) DBW 187	253

CNPs-primed, (j) DBW 187 CNPs-primed + *A. flavus*, (k) DBW 187 Ag-CNPs-primed, (l) DBW 187 Ag-CNPs-primed + *A. flavus*, (m) HI 8759 non-primed, (n) HI 8759 non-primed + *A. flavus*, (o) HI 8759 CNPs-primed, (p) HI 8759 CNPs-primed + *A. flavus*, (q) HI 8759 Ag-CNPs-primed, (r) HI 8759 Ag-CNPs-primed + *A. flavus*.

- Fig. 7.7 Effect of Ag-CNPs and CNPs priming on ten kernel weight of (a) Sonalika, (b) DBW 187 and (c) HI 8759 cultivar, in comparison with non-primed seeds. 254
- Fig. 7.8 Representative wheat plants showing yield/pot of (a) Sonalika non-primed, (b) Sonalika CNPs-primed, (c) Sonalika Ag-CNPs-primed, (d) DBW 187 non-primed, (e) DBW 187 CNPs-primed, (f) DBW 187 Ag-CNPs-primed, (g) HI 8759 non-primed, (h) HI 8759 CNPs-primed, (i) HI 8759 Ag-CNPs-primed. 255
- Fig. 7.9 Effect of Ag-CNPs and CNPs priming on grain yield/pot of (a) Sonalika, (b) DBW 187 and (c) HI 8759 cultivar, in comparison with non-primed seeds. 256
- Fig. 7.10 Effect of Ag-CNPs and CNPs priming on harvest index % of (a) Sonalika, (b) DBW 187 and (c) HI 8759 cultivar, in comparison with non-primed seeds. 257
- Fig. 7.11 Albumin content of harvest wheat seeds from Sonalika, DBW 187 and HI 8759 cultivar under treatment with CNPs and Ag-CNPs, in comparison with non-primed seeds. 260
- Fig. 7.12 Globulin content of harvest wheat seeds from Sonalika, DBW 187 and HI 8759 cultivar under treatment with CNPs and Ag-CNPs, in comparison with non-primed seeds. 260
- Fig. 7.13 Gliadin content of harvest wheat seeds from Sonalika, DBW 187 and HI 8759 cultivar under treatment with CNPs and Ag-CNPs, in comparison with non-primed seeds. 261
- Fig. 7.14 Gluten content of harvest wheat seeds from Sonalika, DBW 187 and HI 8759 cultivar under treatment with CNPs and Ag-CNPs, in comparison with non-primed seeds. 261

Fig. 7.15	Total protein profiling of harvested wheat seeds through SDS-PAGE. (a) Gel image, (b) Scanned image of gel and (c) Relative density of major bands that appeared in the gel.	263
Fig. 7.16	Total protein profiling of harvested wheat seeds (artificially inoculated with <i>A. flavus</i> ) through SDS-PAGE. (a) Gel image, (b) Scanned image of gel and (c) Relative density of major bands that appeared in the gel. [M denotes molecular marker].	264
Fig. 7.17	Seed carbohydrate composition of harvested seeds of Sonalika cultivar nano-primed with Ag-CNPs and CNPs, in comparison with non-primed seeds, both under inoculated and non-inoculated condition.	265
Fig. 7.18	Seed carbohydrate composition of harvested seeds of DBW 187 cultivar nano-primed with Ag-CNPs and CNPs, in comparison with non-primed seeds, both under inoculated and non-inoculated condition.	266
Fig. 7.19	Seed carbohydrate composition of harvested seeds of HI 8759 cultivar nano-primed with Ag-CNPs and CNPs, in comparison with non-primed seeds, both under inoculated and non-inoculated condition.	266
Fig. 7.20	Detection of catalase (CAT) isoforms (a) gel image of isoforms present in uninoculated seeds, (b) scanned image of the gel containing isoforms present in uninoculated seeds, (c) gel image of isoforms present in inoculated seeds, (d) scanned image of the gel containing isoforms present in inoculated seeds, (e) relative density of the isoform present in uninoculated seeds, (f) relative density of the isoform present in inoculated seeds.	268
Fig. 7.21	Detection of peroxidase (POD) isoforms (a) gel image of isoforms present in uninoculated seeds, (b) scanned image of the gel containing isoforms present in uninoculated seeds, (c) gel image of isoforms present in inoculated seeds, (d) scanned image of the gel containing isoforms present in inoculated	269

seeds, (e) relative density of the isoform present in uninoculated seeds, (f) relative density of the isoform present in inoculated seeds.

- Fig. 7.22 Detection of superoxide dismutase (SOD) isoforms (a) gel image of isoforms present in uninoculated seeds, (b) scanned image of the gel containing isoforms present in uninoculated seeds, (c) gel image of isoforms present in inoculated seeds, (d) scanned image of the gel containing isoforms present in inoculated seeds, (e) relative density of the isoform present in uninoculated seeds, (f) relative density of the isoform present in inoculated seeds. 270
- Fig. 7.23 Detection of NADPH oxidase (NOX) isoforms (a) gel image of isoforms present in uninoculated seeds, (b) scanned image of the gel containing isoforms present in uninoculated seeds, (c) gel image of isoforms present in inoculated seeds, (d) scanned image of the gel containing isoforms present in inoculated seeds, (e) relative density of the isoform present in uninoculated seeds, (f) relative density of the isoform present in inoculated seeds. 271
- Fig. 7.24 Detection of Ascorbate peroxidase (APX) isoforms (a) gel image of isoforms present in uninoculated seeds, (b) scanned image of the gel containing isoforms present in uninoculated seeds, (c) gel image of isoforms present in inoculated seeds, (d) scanned image of 273the gel containing isoforms present in inoculated seeds, (e) relative density of the isoform present in uninoculated seeds, (f) relative density of the isoform present in inoculated seeds. 273
- Fig. 7.25 Detection of Polyphenol oxidase (PPO) isoforms (a) gel image of isoforms present in uninoculated seeds, (b) scanned image of the gel containing isoforms present in uninoculated seeds, (c) gel image of isoforms present in inoculated seeds, (d) scanned image of the gel containing isoforms present in 274

inoculated seeds, (e) relative density of the isoform present in uninoculated seeds, (f) relative density of the isoform present in inoculated seeds.

Fig. 7.26	Seed germination percentage of harvested seeds of Sonalika, DBW 187 and HI 8759 cultivar.	275
Fig. 7.27	Assessment of fungal load of harvested seeds from (a,d,g) non-primed, (b,e,h) CNPs-primed and (c,f,i) Ag-CNPs-primed plants of (a-c) Sonalika, (d-f) DBW 187 and (g-i) HI 8759 cultivar.	276
Fig. 7.28	LC-MS chromatogram with base peak intensity (BPI) profiling of metabolic compounds obtained from analysing harvested seeds from Ag-CNPs primed plants.	278
Fig. 7.29	LC-MS chromatogram with base peak intensity (BPI) profiling of metabolic compounds obtained from analysing harvested seeds from non-primed plants.	278
Fig. 7.30	Sun-burst plot presenting metabolites derived from harvested seeds of Ag-CNPs primed plants.	279
Fig. 7.31	Sun-burst plot presenting metabolites derived from seeds of non-primed plants.	280
Fig. 7.32	An overview of wheat seed nano-priming technique with CNPs and Ag-CNPs, in comparison with non-primed seeds, under <i>A. flavus</i> inoculated and uninoculated condition.	291
Fig. 8.1	A conclusive diagram based on the objectives of the thesis.	295